International Journal of Automotive Technology, Vol. 22, No. 2, pp. 489–497 (2021)
DOI 10.1007/s12239–021–0045–z

pISSN 1229–9138/ eISSN 1976–3832

FUEL RAIL PRESSURE CONTROL CHARACTERISTICS OF A GDI HIGH-PRESSURE FUEL PUMP USING A NEWLY DEVELOPED EXPERIMENTAL SYSTEM CONTROLLED WITH A MICROCONTROLLER

Byoung Jin Lee and Choong Hoon Lee*

Department of Mechanical and Automotive Engineering, Seoul National University of Science and Technology, Seoul 01811, Korea

(Received 3 June 2020; Revised 31 July 2020; Accepted 18 August 2020)

ABSTRACT–An experimental system was developed to evaluate the fuel injection parts of a gasoline direct injection engine. An AC motor and an inverter were used to rotate the camshaft in the engine cylinder head. A single plunger high-pressure fuel pump (HPFP) driven by a square cam at the end of the camshaft was used in the gasoline direct injection engine. The rotation position of the square cam was measured by a rotary encoder. The developed system allows control of the camshaft rotation speed, the HPFP pressure control valve (PCV) opening and closing timing, and the fuel injection duration, which are three important factors affecting the fuel rail pressure (FRP). It is confirmed that the fuel rail pressure can be made to vary wit different combinations of these three factors. By using the experimental system developed in this study, the fuel rail pressure can be effectively controlled in the range of 3 MPa to 20 MPa. The most influential factor for control of the fuel rail pressure was the HPFP PCV opening and closing timings. With the proposed using the experimental system, the rail pressure, fuel rail pressure wave characteristics, and the injector drive characteristics can all be assessed under various fuel injection conditions.

KEY WORDS : Gasoline direct injection (GDI), High pressure fuel pump (HPFP), Microcontroller, Fuel rail pressure (FRP), Pressure control valve (PCV)

1. INTRODUCTION

The injection of fuel in a gasoline engine is done mainly by either the PFI (port fuel injection) method or the gasoline direct injection method. In the past, with PFI, mainly low pressures were used. Because the gasoline direct injection method involves the direct injection of fuel into the cylinder, similar to a diesel engine, the fuel injection pressure is controlled and can be as high as 35 MPa (Zhao and Lai, 1997; Husted *et al*., 2014; Golzari *et al.*, 2016; Reddy and Mallikarjuna, 2017; Spakowski *et al.*, 2019). Currently, gasoline direct injection engines are used in most passenger cars because they offer better torque and fuel economy than PFI engines at the same displacement volume (Rivera *et al*., 2010). Despite the excellent fuel economy of gasoline direct injection engines, they have several drawbacks, such as the excessive exhaust of soot due to the direct fuel injection process, difficulty with NOx removal due to the lean control of the air-fuel ratio, noise and vibration problems caused by the reciprocating high pressure fuel pump, and the requirement of a complex fuel injection control system (Zhao, 2009; Wang *et al*., 2014). In recent years, PM (particulate matter) emissions from gasoline direct injection engines have become a problem (Payri *et al*., 2018).

The fuel injection system has the greatest effect on the performance of a gasoline direct injection engine. Compared to the PFI system, which maintains the fuel rail pressure using a single low pressure pump submerged in the fuel tank, gasoline direct injection pressure control is very complex. A low pressure pump, a high pressure fuel pump, a fuel rail and injectors are the key components of the gasoline direct injection system. From the low pressure fuel pump in the fuel tank, the fuel is sent to the inlet to the high pressure fuel pump. The fuel supplied to the high pressure fuel pump is compressed during the upstroke of the high pressure fuel pump reciprocating plunger driven by the square camshaft, and the high pressure fuel is delivered to the fuel rail. At this time, the fuel rail pressure of the gasoline direct injection engine is determined by three factors: the HPFP PCV, camshaft rotation speed, and injector fuel injection duration. In addition, pulsation of the fuel rail pressure is induced during the high pressure fuel delivery process of the HPFP. The fuel rail pressure pulsation causes the injection rate to vary. In addition, the fuel rail pressure pulsation increases the rail pressure amplitude, which

*Corresponding author. e-mail: chlee5@seoultech.ac.kr

results in a failure of the components that make up the injection system, variation of the fuel injection quantity between the cylinders, and noise vibration (Spegar *et al*., 2009; Spegar, 2011; Hiraku *et al*., 2005). The gasoline direct injection system can be evaluated by driving the engine. However, in order to evaluate the fuel injection quantity, fuel rail pressure pulsation, and control condition setting for target rail pressure control under stable experimental conditions, an experimental system is needed to drive the gasoline direct injection system with a motor.

Fuel rail pressure control is the most important task in relation to an evaluation of the gasoline direct injection system. A research on rail pressure control methods with the gasoline direct injection system has been conducted, relying on simulations. Several researchers also directly drove a gasoline direct injection engine to evaluate gasoline direct injection systems (Spegar *et al*., 2009; Spegar, 2011; Hiraku *et al*., 2005). To evaluate such fuel injection systems, a fuel rail pressure control approach similar to the actual engine operating conditions is required. To the authors' knowledge, there is no previous experimental GDI rig which could investigate the rail pressure control according to various control conditions, camshaft rotation speed, GDI PCV opening/closing and fuel injection duration. This paper realizes the experimental system which could which could investigate the rail pressure control according to various control conditions, camshaft rotation speed, GDI PCV opening/closing and fuel injection duration. In the present study, an experimental system that drives the high pressure fuel pump by driving the gasoline direct injection engine camshaft with a motor is developed. In order to control both the opening and closing of the HPFP PCV and the fuel injection timing so that the outcome is identical to that occurring in an actual engine, an encoder is installed to detect the rotation position of the camshaft. Integrated control of the experimental system for the gasoline direct injection system has been studied using a PC and a real time OS FPGA DAQ system (Lee and Lee, 2018). However, integrated control using a PC and a FPGA-DAQ system is costly and challenging to use. In this study, integrated control of an experimental system for a gasoline direct injection system evaluation is implemented with a single microcontroller. With this microcontroller, the cost could be reduced to 1/3000 of that of the 'PC + FPGA' control method. It was also found to be very accurate in terms of fuel injection system timing control, with tests showing that the microcontroller controls the gasoline direct injection system effectively. Evaluation experiments on the gasoline direct injection system were carried out under various injection conditions, and several experimental datasets were compiled. Specifically, a HPFP FRP control map was obtained while varying the HPFP PCV closing/opening angle timing, the fuel injection duration, and the camshaft rotation speed.

2. EXPERIMENTAL SYSTEMS

Figure 1 shows a typical internal GDI HPFP structure for compressing fuel with a single plunger. The GDI HPFP schematic was modified from Spegar *et al*. (2009). The reciprocating movement of the plunger arises due to the rotational movement of the square cam at the end of the camshaft of the engine. Figure 1 (a) shows the fuel intake process in the pumping chamber with the plunger descending. At this stage, the solenoid is deactivated and the control valve plate moves to the right to suck fuel. Figure 1 (b) shows the fuel pressurized stroke in which the solenoid is activated with the control valve plate in close contact with the left side. The halting of fuel pressurization by the high pressure fuel pump can be accomplished by deactivating the solenoid.

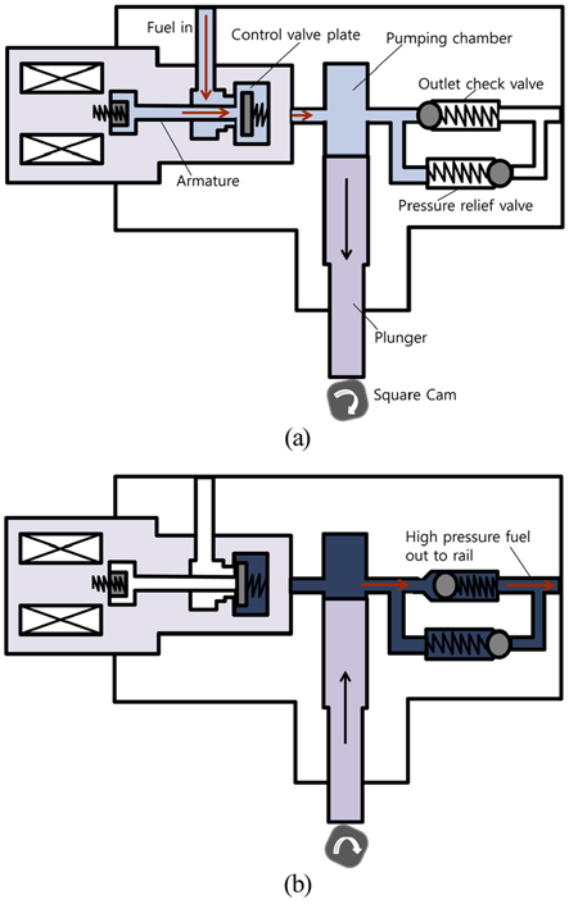

Figure 1. Internal structure of the high pressure fuel pump: (a) fuel intake process with the plunger downward stroke, and (b) pressurization of the fuel with the plunger upward stroke.

Figure 2 shows the experimental system developed for the evaluation of the gasoline direct injection parts. In order to drive the single plunger high pressure fuel pump to mimic actual engine operating conditions, the gasoline direct injection engine cylinder head assembly was separated from the engine cylinder block. The camshaft included in the separated cylinder head assembly was connected to an AC motor through a coupling connection. When the AC motor rotates, the camshaft

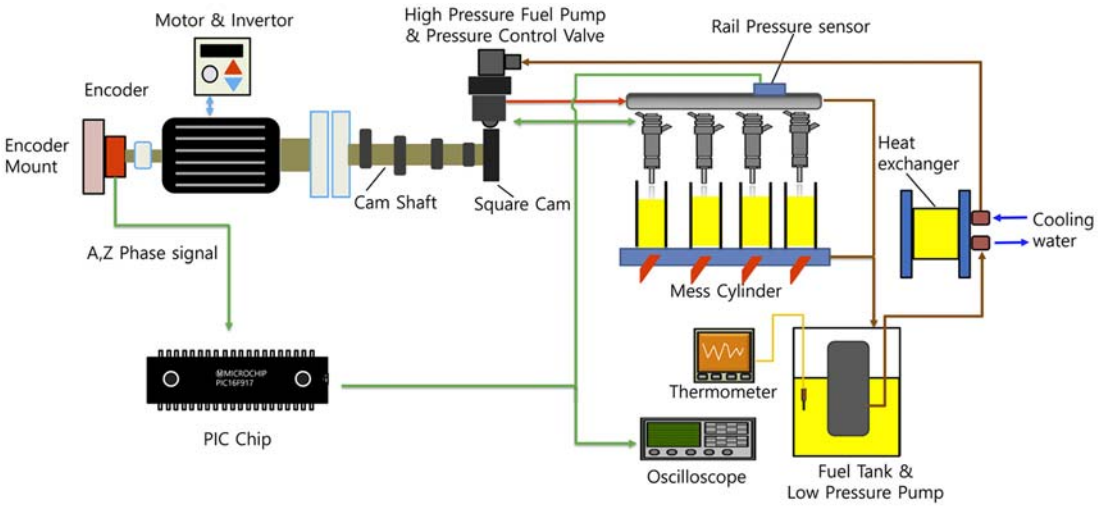

Figure 2. Schematics of the experimental system for evaluating the gasoline direct injection system.

rotates and the square cam at the end of the camshaft reciprocates the single plunger of the high pressure fuel pump.

When the camshaft makes one revolution, the fuel is compressed to a high pressure, four times with the square cam profile, and then sent to the fuel rail. A rotary encoder was mounted on the AC motor shaft to measure the rotation position of the camshaft. One revolution of the rotary encoder produces 360 pulses and has a resolution of 1 degree in terms of the cam angle (CA). The A-phase and Z-phase signals from the rotary encoder were input to the microcontroller to measure the camshaft rotation position. The microcontroller outputs a signal for controlling the opening/closing timing of the HPFP PCV using the camshaft rotation position. The experimental conditions were determined by combining the camshaft rotation speed, the HPFP PCV opening and closing timing, and the fuel injection timing. Under the given experimental conditions, rail pressure sensor signals and the A-phase and Z-phase signals were recorded with a digital oscilloscope. The experiment was repeated 30 times under identical experimental conditions. The fuel temperature has an effect on the fuel injection rate which affect the fuel rail pressure. A heat exchanger was used to keep the fuel temperature constant. By adjusting the amount of cooling water, the fuel tank temperature was kept constant at 30±2 °C. The fuel tank temperature was measured by installing a thermocouple in the fuel tank. When the low pressure fuel pump is driven, fuel with a fuel pressure of 0.4 MPa is supplied to the high pressure fuel pump through the heat exchanger. The fuel injected from the injector was collected into a measuring cylinder and constituted a fuel flow line, which in this case returned the fuel to the fuel tank.

The experimental procedure is summarized as follows. First, we adjust the coolant valve so that the fuel temperature is 30± 2 °C. The inverter knob to set the rotation speed of the AC motor was adjusted, resulting in a constant camshaft rotation speed. The microcontroller programmed the timing interval during which the HPFP PCV closes with a constant cam angle value. The fuel injection duration and injection timing are also programmed to have a constant cam angle. Even if the camshaft rotation speed changes, the HPFP PCV closing period and the injector fuel injection duration are always constant in the cam angle unit. In other words, the solenoid activation timing and deactivation timing of each HPFP PCV and injector are always constant in the cam angle even if the camshaft rotation speed changes. The rail pressure sensor signal, A-phase signals, and Z-phase signals were recorded with a digital oscilloscope at a constant camshaft rotation speed. After changing the camshaft rotational speed, the same experiments were repeated to collect the experimental data.

In the next step, the changes in the HPFP PCV opening and closing timing and the fuel injection timing were newly programmed into the microcontroller and the same experimental processes were repeated.

The HPFP PCV opening angle conditions are ‘BTDC 70 °, BTDC 74 °, BTDC 78 °, BTDC 89 °, and ATDC 10 °’ and the closing angle conditions are ‘BTDC 62 °, BTDC 64 °, BTDC 68 °, and BTDC 70 °’. Experimental conditions combined the

Table 1. Conversion of the fuel injection duration with cam angles at a certain cam shaft rotation speed to ms

Cam angle	400 (rpm)	500 (rpm)	600 rpm	700 (rpm)	800 (rpm)	1000 (rpm)
4°	1.67 (ms)	1.33 (ms)	1.11 (ms)	0.95 (ms)	0.83 (ms)	0.67 (ms)
6°	2.50 (ms)	2.00 (ms)	1.67 (ms)	1.43 (ms)	1.25 (ms)	1.00 (ms)
8°	3.33 (ms)	2.67 (ms)	2.22 (ms)	1.90 (ms)	1.67 (ms)	1.33 (ms)

pressure control valve closing/opening angle. The camshaft rotation speed was six cases of 400, 500, 600, 700, 800 and 1000 rpm (at engine speeds of 800 ~ 2000 rpm). These experimental conditions were chosen because the engine rotation speed is mainly in the range of 700 ~ 2000 rpm when driving the vehicle. The fuel injection period was controlled at 4 °, 6 °, and 8 ° by the camshaft angle. The conversion of the fuel injection period of the cam angle at a certain engine speed to the time scale is summarized in Table 1.

3. EXPERIMENTAL PROCEDURE

Figure 3 shows a conceptual diagram of how the HPFP PCV control signal and the injector drive signal are generated after inputting the encoder signals into the microcontroller. The signals shown here only represent a quarter rotation of the camshaft. The microcontroller used in this study is a Microchip PIC16F917 (Microchip, 2017). When the camshaft makes one revolution, the signals shown in Figure 3 are generated four times, except for the Z-phase signal. The Z-phase signal appears only once during one revolution of the camshaft. The encoder A-phase signal generates 360 pulses when the camshaft makes one revolution. The encoder A-phase signal is input to the microcontroller pulse count pin (RA4 pin) to count the number of pulses. The Z-phase signal detects the reference position of the camshaft. When the Z-phase signal is input to the RB0 pin, an interrupt occurs. The A-phase pulse count register is reset with the Z-phase signal interrupt. Therefore, the A-phase pulse counter starts again from 0 when the interrupt occurs for every revolution of the camshaft, enabling the measurement of the camshaft position. When the encoder A- and Z-phase signals are processed, the outcome is the camshaft rotation position with a resolution of one degree of the cam angle. Using the encoder signal, the HPFP PCV control signal and the injector control signal can be output from the microcontroller at the appropriate timing.

The HPFP PCV control signal and injector control signal were output to the RD5 pin and the RC5 pin, respectively. The power source of the injector drive is DC 60V and an IRFP-4668PBF MOSFET device is used to switch the power source. The HPFP PCV drive power (DC 12V) was switched by the control signal from RD5. A 2N3055 transistor was used to switch the injector drive power source. In this study, injector #2 injects fuel four times per one camshaft revolution for control convenience, which is equivalent to sequential injection of four injectors.

Figure 4 shows an example of how the HPFP PCV control signal, the injector drive signal, and the encoder signals A and Z, from top to bottom, are measured with a digital oscilloscope. Figure 4 (a) shows that four HPFP PCV control signals and injector drive signals are generated per Z-phase signal. Figure 4 (b) shows an enlarged view of the 90 ° (CA) section shown in Figure 4 (a).

Because the high pressure fuel pump drive cam is a square cam, the high pressure fuel pump plunger reaches the top dead center at 90 ° (CA) intervals. The high pressure fuel pump plunger used in this study is assembled such that it reaches the top dead center at 0, 90, 180, and 360 ° (CA).

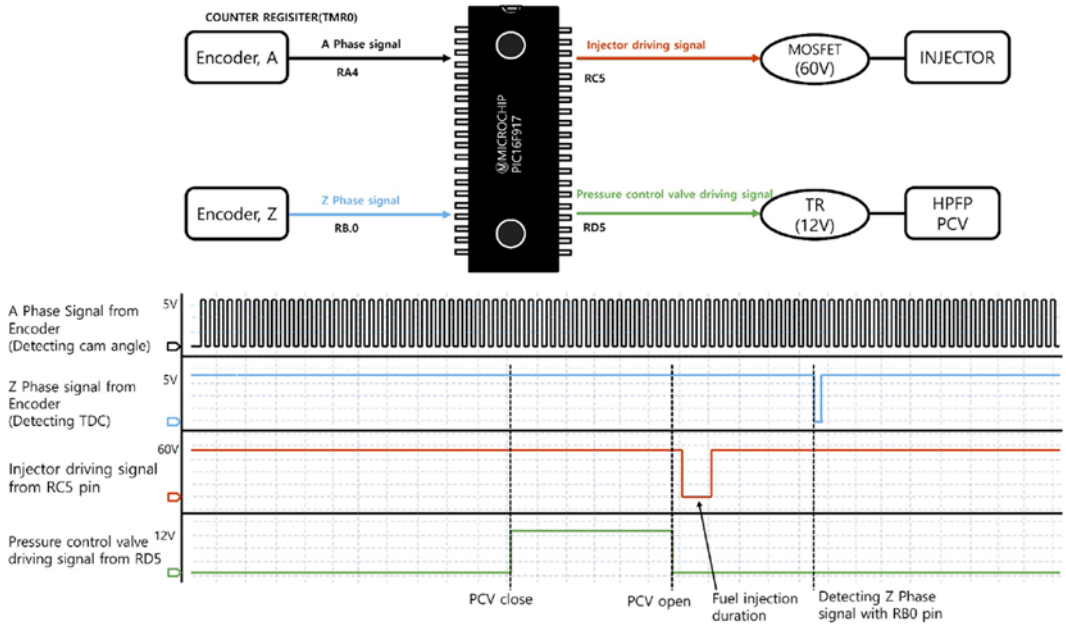

Figure 3. A conceptual diagram of the microcontroller generating the HPFP PCV control signal and the injector drive signal after inputting the encoder A-phase and Z-phase signals into the microcontroller.

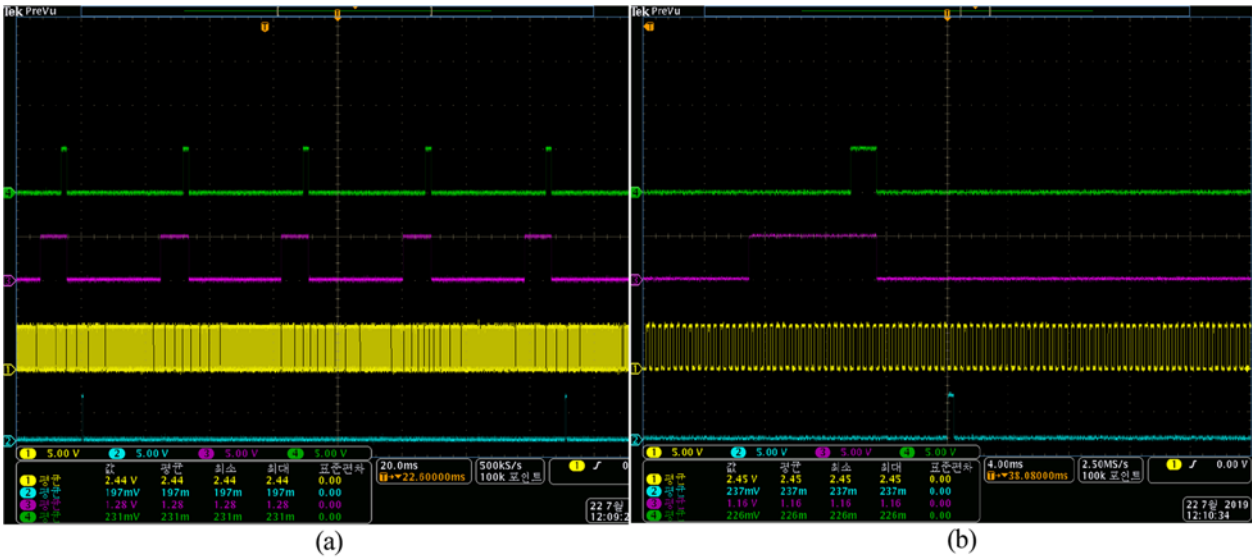

Figure 4. (a) Captured image of the HPFP PCV control signal, the injector drive signal, and the encoder signals A and Z, from top to bottom, with a digital oscilloscope, and (b) magnified image of (a).

4. RESULTS AND DISCUSSION

Figure 5 shows the fuel rail pressure, injector driving voltage and the HPFP PCV driving voltage measured with a digital oscilloscope at a cam shaft rotation speed of 800 rpm, an HPFP PCV close angle of 62 ° (CA), an opening angle of 70 ° (CA) and a fuel injection duration of 2 ° (CA). The close angle of 62 ° (CA) and the opening angle of 70 ° (CA) mean that the HPFP PCV is closed and open at BTDC 28 ° (CA) and BTDC 20 ° (CA), respectively. The FRP signal showed four peaks near BTDC 10 ° (CA). The FRP peak value generally appeared after a certain point of time after the HPFP PCV was opened.

Figure 6 shows the results after measuring the FRP while increasing the camshaft revolution from 400 rpm to 800 rpm in 100 rpm intervals with a HPFP PCV close angle of 62 ° (CA), an opening angle of 70 ° (CA) and an injection duration of 2 ° (CA). This figure shows that the fuel rail pressure varies depending on the change of the camshaft rotation speed. At all camshaft speeds, there were four fuel rail pressure peaks per camshaft revolution. There is a relative delay in the position of the cam angle at which the fuel rail pressure peak appears as the rotational speed increases.

Figures 7 (a) ~ 7 (e) show the average fuel rail pressure according to the camshaft rotation speed when the closing angle is changed from BTDC 62 °, BTDC 64 ° BTDC 66 °, BTDC 68 °, and BTDC 70 ° (denoted correspondingly as C62, C64, C66, C68, and C70 in the Figures 7 (a) ~ 7 (e)) at fixed pressure control valve opening angles of BTDC 70 °, BTDC 74 °, BTDC 78 °, BTDC 89 °, and ATDC 10 °, respectively. Here, C notations in Figures 7a-7e represent close. The fuel

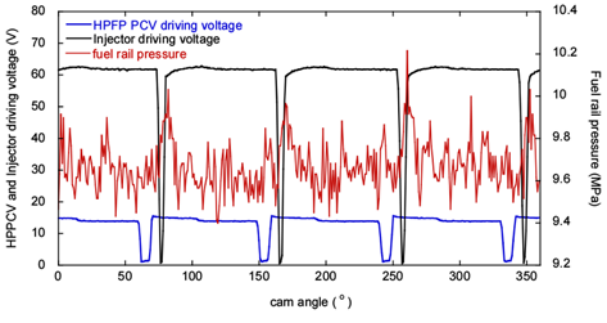

Figure 5. Fuel rail pressure, injector driving voltage, and HPFP PCV signals measured with a digital oscilloscope at a cam shaft rotation speed of 800 rpm.

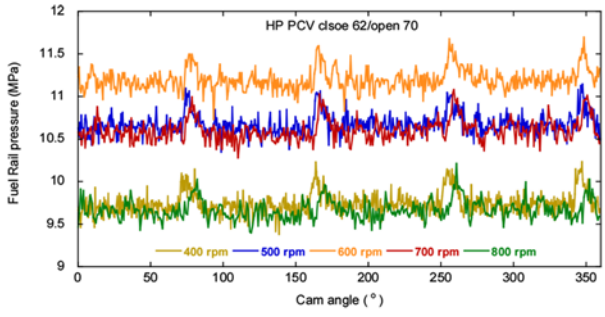

Figure 6. Measurement results of the FRP when increasing the camshaft rotation speed from 400 rpm to 800 rpm in 100 rpm intervals with an HPFP PCV close angle of 62 ° (CA), an opening angle of 70 ° (CA) and an injection duration of 2 ° (CA).

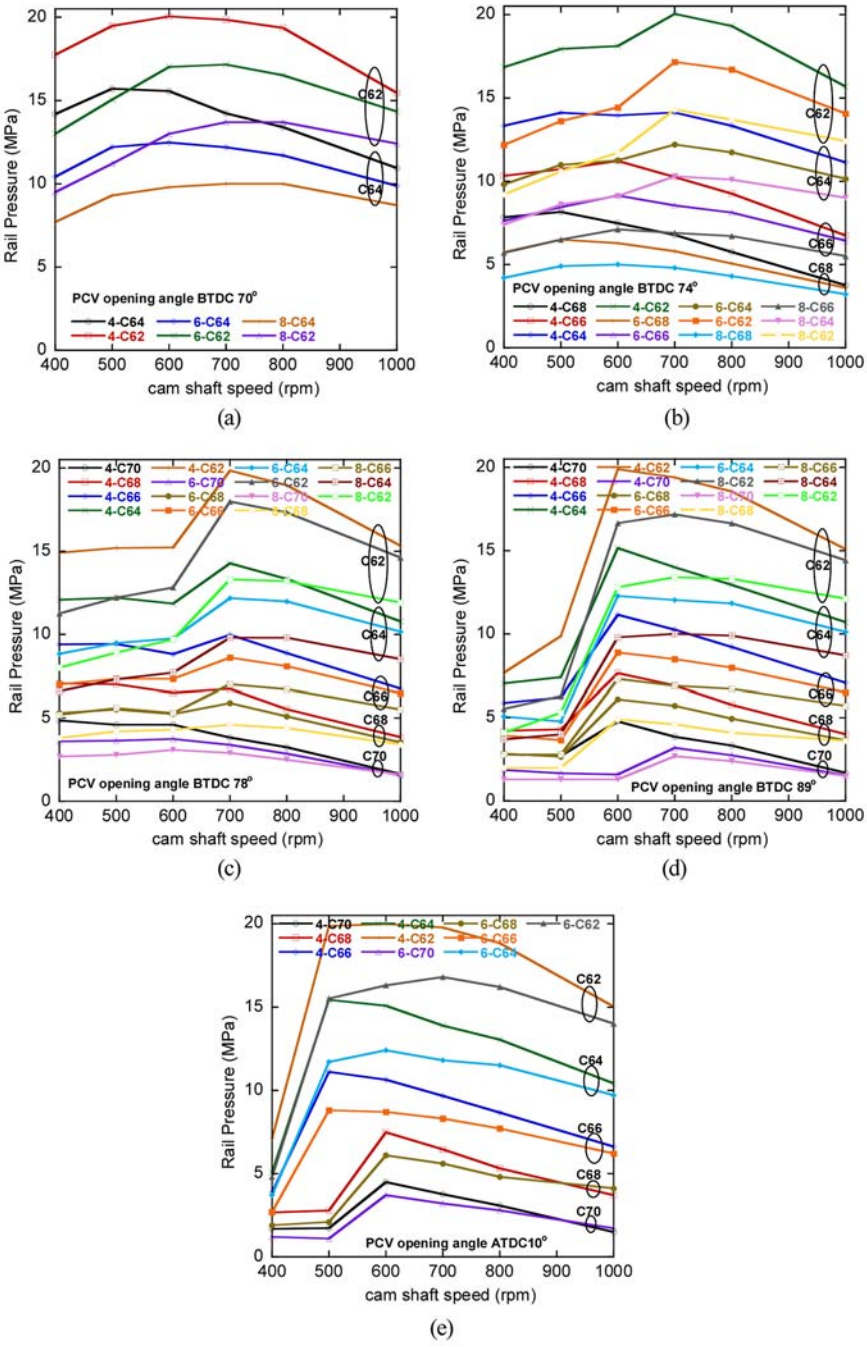

Figure 7. Comparative results of the average FRP obtained for several fixed pressure control valve opening angles while varying the pressure control valve closing angle and the camshaft rotation speed. pressure control valve fixed opening angles: (a) BTDC 70 ° (CA), (b) BTDC 74 ° (CA) (c) BTDC 78 ° (CA), (d) BTDC 89 ° (CA) and (e) ATDC 10 ° (CA).

injection duration was varied in three cases of 4 °, 6 ° and 8 ° of the cam angle. The camshaft rotation speed was changed with six cases of 400, 500, 600, 700, 800, and 1000 rpm. In Figures 7 (a) ~ 7 (e), the average fuel rail pressure increased as the pressure control valve closing time became earlier (as the pressure control valve closing angle decreased) with fixed pressure control valve opening angles. The peak value of the average fuel rail pressure curve according to all pressure control valve opening/closing angle changes was found at the camshaft rotation speed of 600 or 700 rpm. When the fuel injection duration is increased at cam angles of 4 °, 6 °, and 8 °, the average fuel rail pressure decreases. A longer fuel

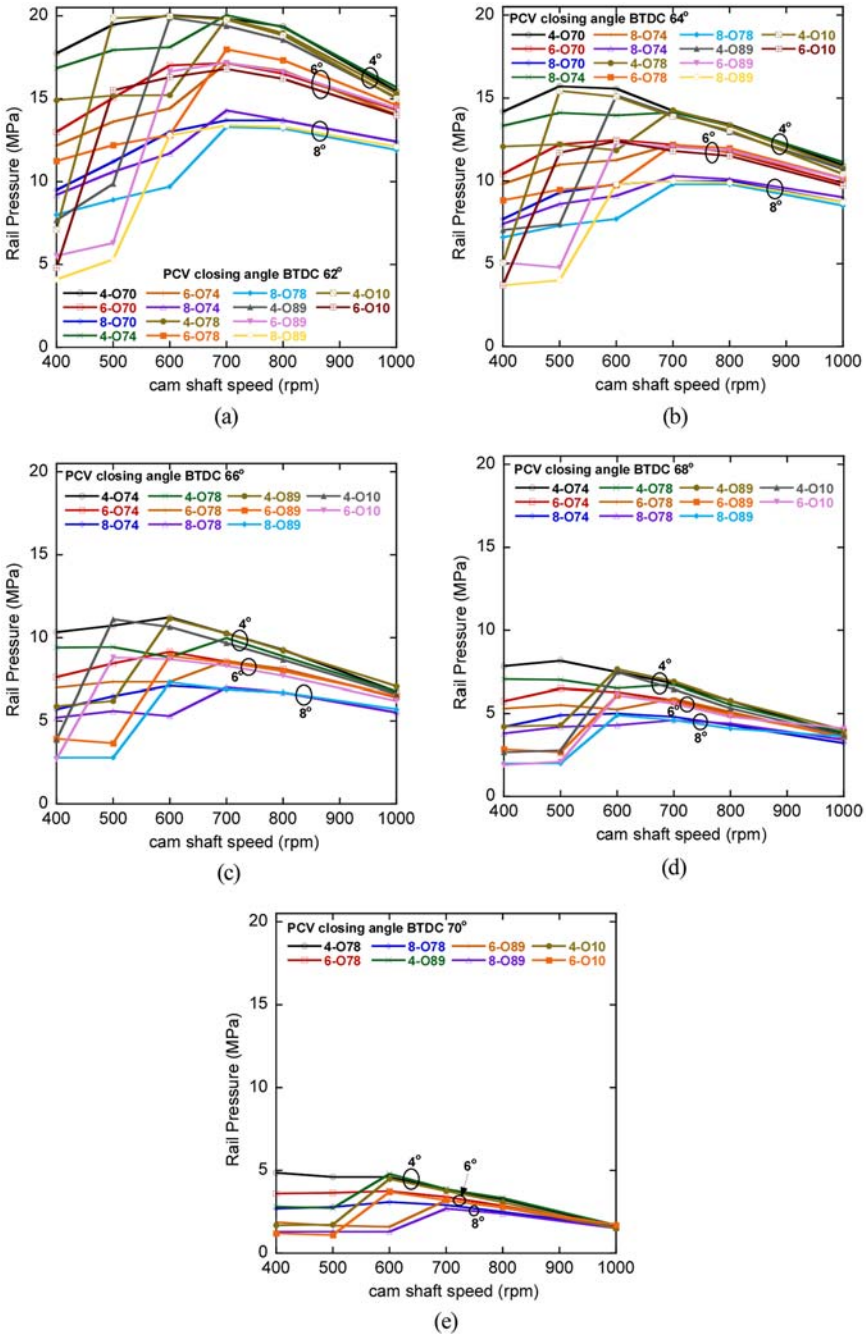

Figure 8. Comparative results of the average FRP obtained for several fixed pressure control valve closing angles while varying the pressure control valve opening angle and the camshaft rotation speed. pressure control valve fixed closing angles: (a) BTDC 62 ° (CA), (b) BTDC 64 ° (CA) (c) BTDC 66 ° (CA), (d) BTDC 68 ° (CA) and (e) BTDC 70 ° (CA).

injection duration, which increases the amount of fuel flowing out of the pressure control valve, decreases the fuel rail pressure. The average fuel rail pressure curve (refer to Figure 7a) at the fixed pressure control valve opening angle of BTDC 70 ° is nearly flat at all camshaft rotation speeds. On the other hand, at the fixed pressure control valve opening angle of ATDC 10 °, the fuel rail pressure curves show a steep slope at 400 ~ 600 rpm. In the range where the fixed pressure control valve opening angle is more retarded, it can be seen that the slope of the fuel rail pressure curve is steeper in the low camshaft rotation speed range. There are no fuel rail pressure curves in the C66, C68, and C70 cases shown in Figure 7 (a)

or in the C66 and C70 cases in Figure 7 (b) due to the insufficient formation of fuel rail pressure in these cases. In these cases, a high fuel rail pressure formed when the camshaft rotation speed was high; however, the fuel rail pressure dropped sharply at a low speed.

Figures 8 (a) ~ 8 (e) show the average fuel rail pressure curves when rearranged with the same data used in Figures 7 (a) ~ 7 (e). That is, the fuel rail pressure curves are displayed with the pressure control valve opening angles varied at a fixed PCV closing angle. Five fixed pressure control valve closing angle cases are BTDC 62 °, BTDC 64 °, BTDC 66 °, BTDC 68 ° and BTDC 70 °. The pressure control valve opening angle is varied at BTDC 70 °, BTDC 74 ° BTDC 78 °, BTDC 89 °, and ATDC 10° (denoted correspondingly as O70, O74, O78, O89, and O10 in Figures 8 (a) ~ 8 (e)) for a fixed PCV closing angle. Figure 8 (a) shows the average fuel rail pressure curves at the fixed pressure control valve closing angle of BTDC 62 ° (the earliest pressure control valve closing case). The average fuel rail pressure curves in Figure 8 (a) show higher values than those in Figure 8 (e) (the most retarded pressure control valve closing case). As the fixed pressure control valve closing angle decreases, the average fuel rail pressure increases. Above the camshaft rotation speed of 700 rpm, the average fuel rail pressure curves in Figures 8 (a) ~ 8 (e) were scarcely affected by the pressure control valve opening angle with the same injection duration. The shorter the fuel injection duration is, the higher the average fuel rail pressure becomes. At camshaft rotation speeds of 600 rpm or less, the lower the camshaft rotation speed is, the greater the effect of the pressure control valve opening angle on the average fuel rail pressure becomes. These results were significantly due to the overlap between the fuel injection timing (BTDC 76 °-BTDC 80 °) and the pressure control valve closing duration, when the camshaft rotation speed was 600 rpm or less. However, in the high-speed of the camshaft rotational speed of 700 ~ 1000 rpm, the larger number of pressurizations by the plunger increases the fuel rail pressure, thus, the effect of the pressure control valve opening timing is small. The implications of the results in Figures 8 (a) ~ 8 (e) can be summarized as follows: fuel rail pressure control at a camshaft speed of 700 rpm or more is mainly possible by controlling the pressure control valve closing angle, and at 700 rpm or less it can be realized by controlling the combination of the pressure control valve closing angle and the opening angle.

The HPFP FRP control map can be obtained by measuring the fuel rail pressure characteristics when the HPFP PCV closing/opening angle timing, the fuel injection duration, and the camshaft rotation speed are varied. Moreover, the variation characteristics of the fuel rail pressure can be determined under each experimental condition. The data obtained from various experimental conditions can be utilized in the design of a gasoline direct injection system. In addition, the developed experimental system is expected to be used when taking measurements of the injector injection rate characteristics under various fuel injection conditions and when testing injector durability.

5. CONCLUSION

An experimental system was developed to evaluate a gasoline direct injection system by driving a gasoline direct injection engine camshaft with an AC motor. A microcontroller was used for integrated control of the experimental system to evaluate the gasoline direct injection system. It was found that various gasoline direct injection systems can be tested and evaluated using the developed experimental system. The following conclusions were obtained.

With the developed experimental system, it was identified that the fuel rail pressure can be controlled in the range of 3 MPa to 20 MPa by controlling the opening/closing timing of the HPFP PCV, the fuel injection timing and the camshaft rotation speed.

An fuel rail pressure control map can be obtained by measuring the FRP characteristics while changing the HPFP PCV closing/opening angle timing, the fuel injection duration, and the camshaft rotation speed.

At a fixed pressure control valve opening angle of the developed gasoline direct injection system, the effect of the closing angle of the pressure control valve on the average fuel rail pressure was significantly affected at all camshaft rotational speeds.

At a fixed pressure control valve closing angle of the developed gasoline direct injection system, the effect of the opening angle of the pressure control valve on the average fuel rail pressure was scarcely affected by the pressure control valve opening angle with the same injection duration when the camshaft rotation speed was 700 rpm or more. At camshaft rotation speeds of 600 rpm or less, the lower the camshaft rotation speed is, the greater the effect of the pressure control valve opening angle on the average fuel rail pressure becomes.

By exposing the developed gasoline direct injection system to various experimental conditions, the design data for a gasoline direct injection could be obtained.

ACKNOWLEDGEMENT–This study was supported by the Research Program funded by the Seoul National University of Science and Technology.

REFERENCES

Golzari, R., Li, Y. and Zhao, H. (2016). Impact of port fuel injection and in-cylinder fuel injection strategies on gasoline engine emissions and fuel economy. *SAE Paper No*. 2016-01-2174.

Hiraku, K., Tokuo, K. and Yamada, H. (2005). Development of high pressure fuel pump by using hydraulic simulator. *SAE Paper No*. 2005-01-0099.

Husted, H., Spegar, T. D. and Spakowski, J. (2014). The effects of GDI fuel pressure on fuel economy. *SAE Paper No*. 2014-01-1438.

Lee, J. M. and Lee, C. H. (2018). A development of fuel rail pressure control system for evaluating GDI injector

performance. *2018 KSAE Annual Spring Conf.*, Busan, Korea.
Microchip Company. (2017). PIC16F917 datasheet.
Payri, R., Bracho, G., Gimeno, J. and Bautista, A. (2018). Rate of injection modelling for gasoline direct injectors. *Energy Conversion and Management*, **166**, 424–432.
Reddy, A. A. and Mallikarjuna, J. M. (2017). Parametric study on a gasoline direct injection engine - A CFD analysis. *SAE Paper No*. 2017-26-0039.
Rivera, E. A., Mastro, N., Zizelman, J., Kirwan, J. and Ooyama, R. (2010). Development of injector for the direct injection homogeneous market using design for six sigma. *SAE Paper No*. 2010-01-0594.
Spakowski, J. G., Kazour, J., Kaswer, B. C., Harstad, M., and Spegar, T. D. (2019). GDI high efficiency fuel pump for fast engine starts and reduced cam loads. *SAE Paper No*. 2019-01-1196.
Spegar, T. D. (2011). Minimizing gasoline direct injection (GDI) fuel system pressure pulsations by robust fuel rail design. *SAE Paper No*. 2011-01-1225.
Spegar, T. D., Chang, S. I., Das, S., Norkin, E. and Lucas, R. (2009). An analytical and experimental study of a high pressure single piston pump for gasoline direct injection (GDi) engine applications. *SAE Paper No*. 2009-01-1504.
Wang C., Xu, H., Herreros, J. M., Wang, J. and Cracknell, R. (2014). Impact of fuel and injection system on particle emissions from a GDI engine. *Applied Energy* **132,** 178–191.
Zhao, F. Q. and Lai, M. C. (1997). A review of mixture preparation and combustion control strategies for spark ignited direct injection gasoline engines. *SAE Paper No*. 970627.
Zhao, F. Q., Lai, M. C. and Harrington, D. L. (1999). Automotive spark ignited direct injection gasoline engines *Progress in Energy and Combustion Science*, **25**, 437–562.
Zhao, H. (2009). *Advanced direct injection combustion engine technologies and development*. Woodhead Publishing Limited.